Hole subbands in strained quantum-well semiconductors in [*hhk*] directions

Guy Fishman
Laboratoire de Spectrométrie Physique, Université Joseph Fourier, Grenoble I, Centre National de la Recherche Scientifique, Boîte Postale 87, 38402 Saint-Martin d'Hères Cedex, France
(Received 14 February 1995)

We give a general formulation for both the Luttinger and the Bir-Pikus Hamiltonians with a spin quantization parallel to the [*hhk*] direction. This allows one to obtain the hole subbands for any growth direction parallel to [*hhk*]. The results are given explicitly in the [001], [111], [110], and [112] directions. We show that the axial approximation is exact if the wave vector parallel to the plane (*hhk*) is equal to zero for (*hhk*)=(001) (a well-known result) or (111) but that this is not strictly true for (110) or (112). We clarify the link between the axial mass and the cyclotron mass. We then present a method of numerical calculation that is suited to any asymmetric quantum well. We discuss the efficiency and the limits of the Broido-Sham transformation and we show that this transformation is not applicable for the [112] direction even as a rough approximation. Finally, we give the hole subband dispersion in strained $Cd_{1-x}Mn_xTe$-CdTe-$Cd_{1-x}Mn_xTe$ quantum wells where, according to the growth direction, the quantum well may or may not be piezoelectric.

I. INTRODUCTION

The hole subband problem in two-dimensional semiconductors (2DSC) was first addressed by Nedorezov[1] who performed the calculation for an infinite square quantum well. The problem was soon solved for quantum wells of different shapes in which the potential includes an electric field but always inside a single semiconductor.[2] In a finite quantum well, where the wave function spreads outside the well, it is necessary to use boundary conditions that take into account the peculiarities of the Luttinger Hamiltonian[3] H_L: this allows one to solve the problem[4–6] in the effective-mass approximation, which is the framework of this paper. Many methods have been proposed depending on the problem of interest.[7–13] The first investigations were related to a [001] growth axis. These were extended to stressed 2DSC (Refs. 14–16) then to strained 2DSC (Refs. 17–19) described by the Bir-Pikus Hamiltonian[20] H_{BP}. The Hamiltonian to be solved is $\mathbf{H}=H_L+H_{BP}+V(z)$ where z is the direction of the growth axis; $V(z)$ defines the quantum well and depends only on the difference in chemical composition between the well and the barrier. The interest in strained semiconductors increased when it was realized that for growth axes other than [001] a piezoelectric field renders the quantum well asymmetric.[19] (Of course asymmetric structures can be created without any electric field.[21,22]) This led to studies of 2DSC most particularly in the [111] directions[19,23] and also in the [112] directions,[24] which have shown theoretically as well as experimentally that the piezelectric coefficient is highly dependent on the strain in CdTe.[23–25] Other low-symmetry directions have also been studied for other purposes.[26–28] The aim of the calculation differs depending on whether one is interested in either the warping[26] or the density of states.[14] In the latter case, where an average is needed, the axial (or "cylindrical") approximation[7,29,30] is particularly suitable. New methods to calculate the hole subbands were introduced and indeed almost each new case so far considered is a particular one.[6,13,16,17,26] A common point in all of these papers is that the growth axes considered are in [*hhk*] directions. The purpose of this paper is to give a general method provided the Hamiltonian used is of the shape **H** given above. For that we use a description of H_L (as well as H_{BP}) as a combination of tensor operators.[30] In doing this, we discard the linear k term that results from either the lack of symmetry inversion in the zinc-blende structure[31] or the strain-induced valence band splitting:[32] this is justified considering the inaccuracy of the Luttinger parameters (see discussion below) in CdTe, to which we apply our results in this paper. In the framework we obtain a general formulation that allows one to perform the same kind of calculation whatever the [*hhk*] direction.

The layout of this paper is as follows: In Sec. II we derive the general formulation[30] of both H_L and H_{BP}, which allows one to obtain these two Hamiltonians regardless of the axis of quantization. In Sec. III we give the general relation that provides H_L+H_{BP} in [*hhk*] directions. The explicit results are given in Sec. IV for [001], [111], [110], and [112]. In Sec. V we discuss the accuracy of the axial approximation, which is used to get the hole subbands, and we show to what extent it is possible to assign an effective mass to a hole subband. In Sec. VI we give the principles of our method of numerical calculation of the hole subbands; i.e., we discuss the modifications of the calculation of Ref. 10, which is well suited to superlattices but not so well to quantum wells; we also discuss the validity of the Broido-Sham transformation,[7] which permits the solution of a real 2×2 matrix instead of the usual complex 4×4 matrix. A summary is given in Sec. VIII. In the Appendix we give the matrix form of the tensors used in Secs. III and IV, which allows one to get H_L+H_{BP} regardless of the direction [*hhk*].

Throughout the paper we take atomic units $\hbar=m_0=1$. The Hamiltonians are hole Hamiltonians.

II. GENERAL FORMALISM

A. Notation

All of the matrices used throughout this paper are of the form:

$$\begin{bmatrix} |\frac{3}{2}\,\frac{3}{2}\rangle & |\frac{3}{2}\,\frac{1}{2}\rangle & |\frac{3}{2}\,-\frac{1}{2}\rangle & |\frac{3}{2}\,-\frac{3}{2}\rangle \\ P+Q & -S & R & 0 \\ -S^* & P-Q & 0 & R \\ R^* & 0 & P-Q & S \\ 0 & R^* & S^* & P+Q \end{bmatrix} \tag{2.1}$$

where the axis of quantization z is arbitrary. The axes Ox, Oy, Oz must be defined with respect to the axes [100], [010], [001] of the crystal. P, Q, R, S are combinations of k_x, k_y, k_z and of the Luttinger parameters γ_1, γ_2, γ_3.

For the wave vectors we shall use $k_\parallel$ and $k_\pm$ defined as $k_\parallel^2=k_x^2+k_y^2$, $k_\pm=k_x\pm ik_y$.

For the Luttinger parameters we define the linear combinations:[30,33]

$$\gamma_\delta=(\gamma_3-\gamma_2)/2 , \tag{2.2a}$$

$$\overline{\gamma}=(\gamma_3+\gamma_2)/2 , \tag{2.2b}$$

$$\gamma_s=(3\gamma_3+2\gamma_2)/5 . \tag{2.2c}$$

We shall see below that γ_s is needed to describe the spherical part of the Hamiltonians (as the notations are not the same in Refs. 7, 30, and 33 we are led to use our own notation). $H[hjk]$ indicates that the Hamiltonian H is written with a z axis of spin quantization parallel to $[hjk]$. This is a short, but convenient, notation and the axes Ox and Oy or, what amounts to the same thing, the usual Euler angles (α,β,γ) must be specified each time. In the following we use mainly $H[hjk]$ or sometimes $H[\alpha,\beta,\gamma]$ when there may be any ambiguity.

B. Luttinger Hamiltonian

The usual Luttinger Hamiltonian is

$$H_L[001]=\tfrac{1}{2}(\gamma_1+\tfrac{5}{2}\gamma_2)k^2-\gamma_2[k_x^2J_x^2+\text{c.p.}] -\gamma_3[k_xk_y(J_xJ_y+J_yJ_x)+\text{c.p.}] . \tag{2.3}$$

In Eq. (2.3) the axes x, y, and z are, respectively, parallel to [001], [010], and [001] as usual. c.p. means circular permutation.

Let us now consider operators such as p_j or J_j $(j=x,y,z)$, denoted Ξ_j. Following Refs. 30 and 33 we introduce now the second-rank tensor operator Ξ of components Ξ_{jk} such as

$$\Xi_{jk}=\tfrac{3}{2}(\Xi_j\Xi_k+\Xi_k\Xi_j)-\delta_{jk}\Xi^2 . \tag{2.4a}$$

Now $[p_x,p_y]=0$ while $[J_x,J_y]=iJ_z$ (and circular permutation) so that the corresponding second-rank tensor operators are

$$P_{jk}=3p_jp_k-\delta_{jk}p^2 , \tag{2.4b}$$

$$J_{jk}=(3/2)(J_jJ_k+J_kJ_j)-\delta_{jk}J^2 . \tag{2.4c}$$

Useful relations can be found in Refs. 33 and 34. In particular these two tensors have vanishing traces.

The second-rank tensor operators can be reduced to irreducible spherical tensors of ranks 0, 1, and 2 denoted $\Xi^{(0)}$, $\Xi^{(1)}$, and $\Xi^{(2)}$. There is one component of $\Xi^{(0)}$ ($\Xi_0^{(0)}$), three components of $\Xi^{(1)}$ ($\Xi 0^{(1)}$, $\Xi_{\pm1}^{(1)}$), and five components of $\Xi^{(2)}$ ($\Xi_0^{(2)}$, $\Xi_{\pm1}^{(2)}$, $\Xi_{\pm2}^{(2)}$). Here we only need $\Xi^{(2)}$ (see the Appendix of Ref. 33 for details on $\Xi^{(0)}$ and $\Xi^{(1)}$),

$$\Xi_0^{(2)}=(\tfrac{3}{2})^{1/2}\Xi_{zz} , \tag{2.4d}$$

$$\Xi_{\pm1}^{(2)}=\mp(\Xi_{xz}\pm i\Xi_{yz}) , \tag{2.4e}$$

$$\Xi_{\pm2}^{(2)}=\tfrac{1}{2}(\Xi_{xx}-\Xi_{yy}\pm 2i\Xi_{xy}) , \tag{2.4f}$$

so that, for example,

$$P_0^{(2)}=(\tfrac{3}{2})^{1/2}(3p_z^2-p^2) , \tag{2.4g}$$

$$P_{\pm1}^{(2)}=\mp 3p_\pm p_z , \tag{2.4h}$$

$$P_{\pm2}^{(2)}=\tfrac{3}{2}p_\pm^2 , \tag{2.4i}$$

with $p_\pm=p_x\pm ip_y$.

The same holds for the second-rank tensor $J^{(2)}$: it is straightforward to write each component of $J^{(2)}$ as a 4×4 matrix.

We now need the scalar product $P^{(2)}\cdot J^{(2)}$ and more generally the tensorial product $P^{(2)}\otimes J^{(2)}$,

$$P^{(2)}\cdot J^{(2)}=P_0^{(2)}J_0^{(2)}-[P_{-1}^{(2)}J_1^{(2)}+P_1^{(2)}J_{-1}^{(2)}] +[P_{-2}^{(2)}J_2^{(2)}+P_2^{(2)}J_{-2}^{(2)}] . \tag{2.4j}$$

It will be useful to use

$$t_s=-\tfrac{1}{9}P^{(2)}\cdot J^{(2)} . \tag{2.4k}$$

In fact we do not need the entire product $P^{(2)}\otimes J^{(2)}$ (one part of which is the scalar product) but only $[P^{(2)}\otimes J^{(2)}]^{(4)}$, which has nine components. These components can be obtained from the Clebsch-Gordan coefficients, namely,

$$T_M=[P^{(2)}\otimes J^{(2)}]_M^4, \quad M=0,\pm1,\pm2,\pm3,\pm4 , \tag{2.5a}$$

$$T_{\pm4}=P_{\pm2}^{(2)}J_{\pm2}^{(2)} , \tag{2.5b}$$

$$T_{\pm3}=2^{-1/2}[P_{\pm2}^{(2)}J_{\pm1}^{(2)}+P_{\pm1}^{(2)}J_{\pm2}^{(2)}] , \tag{2.5c}$$

$$T_{\pm2}=7^{-1/2}[(\tfrac{3}{2})^{1/2}P_{\pm2}^{(2)}J_0^{(2)}+2P_{\pm1}^{(2)}J_{\pm1}^{(2)} +(\tfrac{3}{2})^{1/2}P_0^{(2)}J_{\pm2}^{(2)}] , \tag{2.5d}$$

$$T_{\pm1}=7^{-1/2}[2^{-1/2}P_{\pm2}^{(2)}J_{\mp1}^{(2)}+3^{1/2}P_{\pm1}^{(2)}J_0^{(2)} +3^{1/2}P_0^{(2)}J_{\pm1}^{(2)}+2^{-1/2}P_{\mp1}^{(2)}J_{\pm2}^{(2)}] , \tag{2.5e}$$

$$T_0=(70)^{-1/2}[P_2^{(2)}J_{-2}^{(2)}+4P_1^{(2)}J_{-1}^{(2)}+6P_0^{(2)}J_0^{(2)} +4P_{-1}^{(2)}J_1^{(2)}+P_{-2}^{(2)}J_2^{(2)}] . \tag{2.5f}$$

It will be useful to use t_0 and t_M defined by

$$t_0=(\sqrt{70}/9)T_0 , \tag{2.5g}$$

$$t_M=\tfrac{1}{9}(T_M-T_{-M}),\quad M=1,3 \tag{2.5h}$$

$$t_M=\tfrac{1}{9}(T_M+T_{-M}),\quad M=2,4\ . \tag{2.5i}$$

All of the tensors (t_s and the t_M) needed to write the Hamiltonians as matrices are given in the Appendix.

We now introduce a "spherical" Hamiltonian H_s, which does not depend on the axes:

$$H_s=\tfrac{1}{2}\gamma_1 k^2+\gamma_s t_s\ , \tag{2.6}$$

so that the usual Luttinger Hamiltonian is

$$H_L[001]=H_s+\gamma_\delta[c_0t_0+c_4t_4]\ , \tag{2.7a}$$

with

$$c_0=\tfrac{1}{5},\quad c_4=1\ . \tag{2.7b}$$

In this case,

$$P=\tfrac{1}{2}\gamma_1 k^2\ , \tag{2.8a}$$

$$Q=\tfrac{1}{2}\gamma_2(k_\parallel^2-2k_z^2)\ , \tag{2.8b}$$

$$R=(\sqrt{3}/2)(-\bar{\gamma}k_-^2+\gamma_\delta k_+^2)\ , \tag{2.9a}$$

$$S=\sqrt{3}\gamma_3 k_z k_-\ . \tag{2.9b}$$

A very useful approximation is the axial approximation. This approximation can be understood in two ways. The first[7,8] is to assume $\gamma_\delta=0$ only in Eq. (2.9a) (which does not mean that $\gamma_2=\gamma_3$ elsewhere), the second[30] is to make $c_4=0$ in Eq. (2.7b). These two methods are identical in [001] directions and amount to neglect of the warping in the (k_x,k_y) plane: this is straightforward in the first method; the advantage of the second, however, is that it is possible to generalize this approximation in other directions.[30]

C. Bir-Pikus Hamiltonian

The usual Bir-Pikus Hamiltonian $H_{BP}[001]$ is[20]

$$H_{BP}[001]=-a\sum_i \varepsilon_{ii}-b\sum_i \varepsilon_{ii}[J_i^2-\tfrac{1}{3}J^2]-\frac{2d}{\sqrt{3}}\left[\varepsilon_{xy}\frac{J_xJ_y+J_yJ_x}{2}+\text{c.p.}\right]\ . \tag{2.10}$$

We define

$$\beta_1=-2a,\quad \beta_2=b,\quad \beta_3=d/\sqrt{3}\ , \tag{2.11}$$

so that

$$H_{BP}[001]=\tfrac{1}{2}[\beta_1+\tfrac{5}{2}\beta_2]\sum_i \varepsilon_{ii}-\beta_2\sum_i \varepsilon_{ii}J_i^2-\beta_3[\varepsilon_{xy}(J_xJ_y+J_yJ_x)+\text{c.p.}] \tag{2.12}$$

and

$$H_{BP}[001]=\tfrac{1}{2}\beta_1\sum_i \varepsilon_{ii}+\beta_s\tau_s+\beta_\delta[\tfrac{1}{5}\tau_0+\tau_4]\ , \tag{2.13}$$

where the only difference between t_M and τ_M is that k_ik_j in t_M has to be replaced by ε_{ij} in τ_M. β_s and β_δ are similar to γ_s and γ_δ and are defined by Eqs. (2.2a) and (2.2c) where γ is to be replaced by β.

In the same way $H_{BP}[001]$ may be obtained from Eqs. (2.7a) and (2.7b) by changing γ to β.

III. LUTTINGER AND BIR-PIKUS HAMILTONIANS IN [*hhk*] DIRECTIONS

A. [*hkl*] directions

In the general case $H_L[hkl]$ reads

$$H_L[hkl]=H_s+\gamma_\delta\left[\sum_{M'=-4}^{4}C_{M'}(hkl)T_{m'}\right]\ , \tag{3.1}$$

where $T_{M'}$ are operators quantized along the axis $[hjk]$ while in Eq. (2.7a) T_M is quantized along [001].

The new axes can be defined by the Euler angles (α,β,γ) and[34]

$$T_M[001]=\sum_{M'=-4}^{4}T_{M'}R^4_{M'M}(-\gamma,-\beta,-\alpha)\ , \tag{3.2}$$

where $R^4_{MM'}(\alpha,\beta,\gamma)$ is the matrix representing the (α,β,γ) rotation in the $J=4$ representation and is given by

$$R^4_{MM'}(\alpha,\beta,\gamma)=\exp(-i\alpha M)r^4_{MM'}(\beta)\exp(-i\gamma M')\ , \tag{3.3}$$

$r^J_{MM'}(\beta)$ is a function of $\xi=\cos\beta/2$ and $\eta=\sin\beta/2$ given in Ref. 34. Finally,

$$T_M[001]=\left[\sum_{M'=-4}^{4}T_{M'}e^{i\gamma M'}r^4_{M'M}(-\beta)\right]e^{i\alpha M}\ . \tag{3.4}$$

Equation (2.7a) then allows one to obtain $H_L[hkl]$ as a function of $T_{M'}[hkl]$.

We note that our formulation is very near but not identical to the one of Ref. 30 where the authors rotate the operators while it is more convenient in our case to have the axes rotated. The framework being given, we now deal more precisely with the [*hhk*] directions.

B. [*hhk*] directions

The [*hhk*] directions define a new axis of quantization (z axis) but the new axes x and y are still to be defined. An initial idea might be to rotate the axes so that *Ox* and *Oy* are symmetric with respect to the $(1\bar{1}0)$ plane: then *Ox* and *Oy* play the same role. This can be performed using results from Ref. 35 for the [111] direction and is an appropriate method if there is no strain. However, when the strain has to be taken into account this leads to numerous nonzero strain tensor components ε_{ij}. In order to use the fact that the $(1\bar{1}0)$ plane is a symmetry plane when the growth direction is [*hhk*] it is preferable to put the x axis in the $(1\bar{1}0)$ plane: this maximizes the number of zeros in the strain tensor[24] ε_{ij} and in fact, for $i\neq j$, only the term ε_{xz} can be nonzero. The y axis is then determined. For the usual Euler angles (α,β,γ) this amounts to taking

$$\alpha=\pi/4\ ,\qquad \beta=\arccos[k(k^2+2h^2)^{-1/2}],\quad \gamma=0\ . \tag{3.5}$$

From now on we keep these values for α, β, and γ. Using the definitions of Sec. II and the equations of paragraph III A, a lengthy calculation shows the Luttinger Hamiltonian $H_L[hhk]$ now reads as

$$H_L[hhk]=H_s+\gamma_\delta\left[\sum_{M=0}^{4} c_M t_M\right], \tag{3.6a}$$

with

$$c_0=\tfrac{1}{5}(1+60\xi^4\eta^4-20\xi^2\eta^2), \tag{3.6b}$$

$$c_1=2\sqrt{14}\xi\eta(\xi^2-\eta^2)(1-6\xi^2\eta^2), \tag{3.6c}$$

$$c_2=4\sqrt{7}\xi^2\eta^2(1-6\xi^2\eta^2), \tag{3.6d}$$

$$c_3=2\sqrt{2}\varepsilon\eta(\xi^2-\eta^2)(1+6\xi^2\eta^2), \tag{3.6e}$$

$$c_4=12\xi^4\eta^4+4\xi^2\eta^2-1. \tag{3.6f}$$

The set of Eq. (3.6), which gives explicitly H_L, is the keystone to obtain Hamiltonians for a growth direction parallel to $[hhk]$. With the matrices given in the Appendix, this set allows one to obtain any Hamiltonian of interest here by a straightforward calculation. For example, Table I gives the coefficient c_M in four directions. Incidently we can note that c_4, which is equal to -1 in Table I, is not identical to the coefficient c_4 (which is equal to 1) of Eq. (2.7); this results only from the fact that the new y axis is no longer parallel to [010] and thus the phase is not the same. The axial approximation here amounts to make $c_M=0$ for $M>0$: only the first term c_0 is kept.

In the same way the Bir-Pikus Hamiltonian now reads with the same notation:

$$H_{BP}[hhk]=\tfrac{1}{2}\beta_1\sum_i \varepsilon_{ii}+\beta_s\tau_s+\beta_\delta\left[\sum_{M=0}^{4} c_M\tau_M\right]. \tag{3.7}$$

Of course, the axial approximation has no meaning for the Bir-Pikus Hamiltonian and we must keep all the terms.

Finally we can wonder if the above method, summarized in Eqs. (3.6) and (3.7), is applicable when the spin-orbit splitting Δ is weak (as, for example, in silicon) or in other words when both bands Γ_8 and Γ_7 are to be taken into account simultaneously. First, if Δ equals zero (spin-orbit interaction neglected), the above method is applicable [see Eq. (16) of Ref. 33]. Second, if Δ does not equal zero, it is not possible to write the whole Hamiltonian describing $\Gamma_8+\Gamma_7$ as a sum of tensor operators and therefore to obtain a set of equations like Eqs. (3.6) and (3.7). It is still possible to use the axial approximation for a growth direction parallel to [001] but not for other directions: this results mainly from the fact that the Hamiltonian describing the axial approximation in $[hhk]$ directions cannot be deduced from the Hamiltonian describing the axial approximation in the [001] direction by a simple rotation.

We have now the framework to calculate the Hamiltonians. In the following we give the matrix elements of $H_L[hhk]+H_{BP}[hhk]$.

IV. MATRIX ELEMENTS

We first give the matrix elements of $H_L[hhk]$ and then those of $H_{BP}[hhk]$; the potential problem is briefly considered at the end of this section. It is understood that the phases are defined by Eq. (3.5).

In these matrix elements the following linear combination of Luttinger parameters,

$$\gamma_{np}=(n\gamma_3+p\gamma_2)/(n+p), \tag{4.1}$$

is useful. The Eqs. (2.2b) and (2.2c) are the most important particular cases of Eq. (4.1).

A. Matrix elements of H_L

[001] direction:

$$P\pm Q=\tfrac{1}{2}(\gamma_1\mp 2\gamma_2)k_z^2+\tfrac{1}{2}(\gamma_1\pm\gamma_2)k_\parallel^2, \tag{4.2a}$$

$$R=-(\sqrt{3}/2)\overline{\gamma}k_-^2-(\sqrt{3}/2)\gamma_\delta k_+^2, \tag{4.2b}$$

$$S=\sqrt{3}\gamma_3 k_- k_z. \tag{4.2c}$$

[111] direction:

$$P\pm Q=\tfrac{1}{2}(\gamma_1\mp 2\gamma_3)k_z^2+\tfrac{1}{2}(\gamma_1\pm\gamma_3)k_\parallel^2, \tag{4.3a}$$

$$R=-(\sqrt{3}/2)\gamma_{21}k_-^2-(4/\sqrt{6})\gamma_\delta k_+ k_z, \tag{4.3b}$$

$$S=\sqrt{3}\gamma_{12}k_- k_z+(\sqrt{2/3})\gamma_\delta k_+^2. \tag{4.3c}$$

[110] direction:

TABLE I. This table gives the coefficient C_M, which allows one to obtain both the Luttinger Hamiltonian and the Bir-Pikus Hamiltonian for the given direction of quantization. The Euler angles are $\alpha=\pi/4$, β, $\gamma=0$. The axial approximation, valid for the Luttinger Hamiltonian, amounts to taking $c_M=0$ for $M>0$. The formulation for a general direction $[hhk]$ is given in the text [see Eq. (3.6)].

$[hhk]$	[001]	[111]	[110]	[112]
c_0	1/5	$-2/15$	$-1/20$	$-1/20$
c_1	0	0	0	$\sqrt{7}/3$
c_2	0	0	$-\sqrt{7}/2$	$\sqrt{7}/6$
c_3	0	4/3	0	1
c_4	-1	0	3/4	$-7/12$

$$P\pm Q=\tfrac{1}{2}(\gamma_1\mp 2\gamma_{31})k_z^2+\tfrac{1}{2}(\gamma_1\pm\gamma_{31})k_\parallel^2 \mp\tfrac{3}{4}\gamma_\delta(k_x^2-k_y^2)\ , \tag{4.4a}$$

$$R=-(\sqrt{3}/2)\gamma_{53}k_-^2+(\sqrt{3}/4)\gamma_\delta[k_\parallel^2-2k_z^2+\tfrac{3}{2}k_+^2]\ , \tag{4.4b}$$

$$S=\sqrt{3}\bar{\gamma}k_-k_z+\sqrt{3}\gamma_\delta k_+k_z\ . \tag{4.4c}$$

[112] direction:

$$P\pm Q=\tfrac{1}{2}(\gamma_1\mp 2\gamma_{31})k_z^2+\tfrac{1}{2}(\gamma_1\pm\gamma_{31})k_\parallel^2 \pm\gamma_\delta[-\sqrt{2}k_xk_z+\tfrac{1}{4}(k_x^2-k_y^2)]\ , \tag{4.5a}$$

$$R=-(\sqrt{3}/2)\gamma_{53}k_-^2 +\gamma_\delta[(1/\sqrt{6})k_-k_z-(\sqrt{3}/12)(k_\parallel^2-2k_z^2) -(\sqrt{3/2})k_+k_z-7\sqrt{3}/24k_+^2]\ , \tag{4.5b}$$

$$S=\sqrt{3}\bar{\gamma}k_-k_z+\gamma_\delta\{-(1/\sqrt{6})[k_\parallel^2-2k_z^2+\tfrac{1}{2}k_-^2] -(1/\sqrt{3})k_+k_z+(\sqrt{3/8})k_+^2\}\ . \tag{4.5c}$$

In Eqs. (4.2)–(4.5) the axial approximation is obtained with $\gamma_\delta=0$. In this approximation $k_+=k_-=k_\parallel$.

B. Matrix elements of H_{BP}

We need the ε_{ij} components for each direction. We write

$$\varepsilon_{xx}=\varepsilon_{yy}=\varepsilon_\parallel,\quad \varepsilon_\perp=\varepsilon_{zz},\quad \varepsilon_{\parallel\perp}=\varepsilon_\parallel-\varepsilon_\perp\ . \tag{4.6}$$

Only the $\varepsilon_\parallel$ component is given by the composition. We deal in this paper with a strained CdTe well and unstrained CdMnTe barriers so that

$$\varepsilon_\parallel=[a(\mathrm{Cd}_{1-x}\mathrm{Mn}_x\mathrm{Te})-a(\mathrm{CdTe})]/a(\mathrm{CdTe}) \tag{4.7}$$

[where $a(X)$ is the cell parameter of the X compound]. The other components ε_{ij} of the strained tensors depend on the direction and are given below.[24,36,37] However, with the Euler angles used only $\varepsilon_\parallel$, $\varepsilon_\perp$, and ε_{xz} may be nonzero. ε_{xy} and ε_{zy} are always zero. We use Eq. (3.6) where γ and t_M are to be replaced by β and τ_M. β_{np} is the same function of β_3 and β_2 as γ_{np} is of γ_3 and γ_2 [see Eq. (4.1)].

Furthermore we give the linear relations between $\varepsilon_\perp$ and ε_{xz} as a function of $\varepsilon_\parallel$. Strain tensor components that are not given below are zero. C_{ij} are elastic stiffness constants.

[001] direction:

$$(P\pm Q)_{BP}=\tfrac{1}{2}[\beta_1(2\varepsilon_\parallel+\varepsilon_\perp)]\pm\beta_2\varepsilon_{\parallel\perp}\ , \tag{4.8a}$$

$$R_{BP}=S_{BP}=0\ , \tag{4.8b}$$

$$\varepsilon_\perp=-(2C_{12}/C_{11})\varepsilon_\parallel\ . \tag{4.8c}$$

[111] direction:

$$(P\pm Q)_{BP}=\tfrac{1}{2}[\beta_1(2\varepsilon_\parallel+\varepsilon_\perp)]\pm\beta_3\varepsilon_{\parallel\perp}\ , \tag{4.9a}$$

$$R_{BP}=S_{BP}=0\ , \tag{4.9b}$$

$$\varepsilon_\perp=-2(C_{11}+2C_{12}-2C_{44})/(C_{11}+2C_{12}+4C_{44})\varepsilon_\parallel\ . \tag{4.9c}$$

[110] direction:

$$(P\pm Q)_{BP}=\tfrac{1}{2}[\beta_1(2\varepsilon_\parallel+\varepsilon_\perp)]\pm\beta_{31}\varepsilon_{\parallel\perp}\ , \tag{4.10a}$$

$$R_{BP}=(\sqrt{3}/2)\beta_\delta\varepsilon_{\parallel\perp}\ , \tag{4.10b}$$

$$S_{BP}=0\ , \tag{4.10c}$$

$$\varepsilon_\perp=(2C_{44}-C_{11}-3C_{12})/(C_{11}+C_{12}+2C_{44})\varepsilon_\parallel\ . \tag{4.10d}$$

[112] direction:

$$(P\pm Q)_{BP}=\tfrac{1}{2}[\beta_1(2\varepsilon_\parallel+\varepsilon_\perp)] \pm(\beta_{31}\varepsilon_{\parallel\perp}-\sqrt{2}\beta_\delta\varepsilon_{xz})\ , \tag{4.11a}$$

$$R_{BP}=-\beta_\delta(\sqrt{2/3}\varepsilon_{xz}+\sqrt{3}/6\varepsilon_{\parallel\perp})\ , \tag{4.11b}$$

$$S_{BP}=\sqrt{3}\beta_{12}\varepsilon_{xz}-\sqrt{2/3}\beta_\delta\varepsilon_{\parallel\perp}\ . \tag{4.11c}$$

Now we need to introduce

$$D_{112}=\tfrac{8}{9}\{13C_{11}C_{44}-7C_{12}C_{44}-4(C_{12})^2 +2[(C_{44})^2+(C_{11})^2+C_{11}C_{12}]\}\ , \tag{4.11d}$$

so that

$$\varepsilon_\perp=[1-16(C_{11}+2C_{12})(C_{11}-C_{12}+C_{44})/(3D_{112})]\varepsilon_\parallel\ , \tag{4.11e}$$

and

$$\varepsilon_{xz}=[4\sqrt{2}(C_{11}+2C_{12})(2C_{44}-C_{11}+C_{12})/(3D_{112})]\varepsilon_\parallel\ . \tag{4.11f}$$

C. Potential

The entire Hamiltonian is $H_L+H_{BP}+V(z)$ where $V(z)$ is the potential due to both the valence band offset and the piezoelectric potential. $V(z)$, which is a scalar, is diagonal regardless of basis. In unstrained semiconductors $V(z)$ describes only the valence band offset. P_{BP} merely induces a shift from $V(z)$. Q_{BP} induces a splitting so that the well for light holes is not the same as for heavy holes. Furthermore H_{BP} is in general not diagonal; strictly speaking, when the strain is not zero and differs in the well and the barrier, the whole potential, which results from both the chemical potential and the potential induced by the strain, is not diagonal. The valence band edge does not correspond to the same wave function in the well and in the barrier: it is not possible to define, even for $k_\parallel=0$, a quantum well in which the wave function of the valence band edge is the same inside and outside the quantum well. Of course if we deal with an energy level, this level is the same throughout the sample and the wave function is well determined. In this sense the [112] direction, and not the three other cases studied

here, is representative of the general case. Finally if there is no strain either in the well or in the barrier we recover the simple case.

V. ACCURACY AND VALIDITY OF THE AXIAL APPROXIMATION

A. Accuracy for $k_{\parallel}=0$

It is well known[8] that the axial approximation is exact for $k_{\parallel}=0$ in the [001] direction. Let us consider what happens in other directions. In this section P (P_A) is the matrix element of H_L without (with) axial approximation. The same applies for Q (Q_A) and R (R_A).

[001] direction:

$$P\pm Q=\tfrac{1}{2}(\gamma_1\mp 2\gamma_2)k_z^2=P_A\pm Q_A\ , \tag{5.1a}$$

$$R=S=0=R_A=S_A\ . \tag{5.1b}$$

We are now in a position to calculate hole subbands for a [001] growth axis (the parameters used are given below in Sec. VI D). We take a CdTe quantum well whose width is 100 Å with a barrier made up with unstrained $Co_{0.8}Mn_{0.2}Te$, which induces strain in CdTe. We keep these values ($L_w=100$ Å, $x=0.2$) throughout this paper. Whatever the direction the well depth is slightly larger than 100 meV (typically 105 meV). Results are given in Fig. 1 for [001] growth axes. In the CdTe quantum well the strain induces a light-hole–heavy-hole splitting V_L-V_H (qualitatively drawn in the inset) equal to 23.9 meV. We have also fitted (parabolic) curves with given masses. There is no exact definition for this kind of curve. Our aim was to find a mass that can be used in an exciton calculation: in such a case the parabolic description is valid up to about the inverse of the Bohr radius, namely, 0.02 Å^{-1} in CdTe. We obtain $m=0.20$ and 0.55 for $H1$ and $H2$, respectively. As usual H and L mean the wave functions are pure $|\frac{3}{2}\pm\frac{3}{2}\rangle$ and $|\frac{3}{2}\pm\frac{1}{2}\rangle$ at $k_{\parallel}=0$. The so-called diagonal masses [see Eq. (4.2a)], $1/(\gamma_1\pm\gamma_2)$, are, respectively, 0.16 and 0.30.

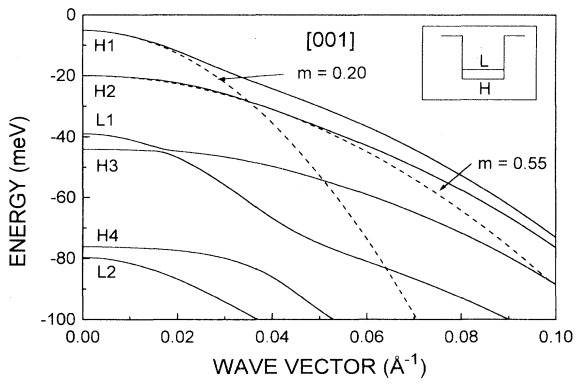

FIG. 1. Energy of the valence subbands in the axial approximation for a $Cd_{0.8}Mn_{0.2}Te$-CdTe-$Cd_{0.8}Mn_{0.2}Te$ quantum well whose growth axis is [001]. The width of the CdTe quantum well is $L_w=100$ Å. All of the other parameters (Luttinger parameters, etc.) are given in the text. This quantum well has no piezoelectric field. Hn and Ln have the usual meaning and correspond, respectively, to pure $|\frac{3}{2}\pm\frac{3}{2}\rangle$ and $|\frac{3}{2}\pm\frac{1}{2}\rangle$ functions at $k_{\parallel}=0$. The splitting V_L-V_H between the valence band edge of the light hole and the heavy hole inside the quantum well is 23.9 meV. The masses $m=0.20$ and 0.55 (in free electron mass units) are obtained by fitting the $H1$ and $H2$ hole subbands up to about 0.02 Å^{-1} and can be used as in-plane masses for $E1$-$H1$ and $E1$-$H2$ excitons. It is hazardous to try to derive a mass for $L1$. The so-called diagonal mass is 0.16 for heavy holes and 0.30 for light holes.

[111] direction:

$$P\pm Q=\tfrac{1}{2}(\gamma_1\mp 2\gamma_3)k_z^2=P_A\pm Q_A\ , \tag{5.2a}$$

$$R=S=0=R_A=S_A\ . \tag{5.2b}$$

Figure 2 gives the hole subbands for the [111] growth axis. There is a strong piezoelectric field and the potential is no longer "flat" inside the well. Indeed this piezoelectric field induces a difference of 120 meV between the two sides of the quantum well; this difference is larger than the well depth. $V_L-V_H=32.2$ meV. For the same conditions as in Fig. 1 we obtain masses equal to 0.20 and 0.38 for $H1$ and $H2$ subbands. The mass 0.20 for $H1$ was used in Ref. 24 for a variational exciton calculation. The diagonal masses [see Eq. (4.3a)], $1/(\gamma_1\pm\gamma_3)$, are, respectively, 0.15 and 0.34.

[110] direction:

$$P\pm Q=\tfrac{1}{2}(\gamma_1\mp 2\gamma_{31})k_z^2=P_A\pm Q_A\ , \tag{5.3a}$$

$$R=-(\sqrt{3}/2)\gamma_\delta k_z^2\ , \tag{5.3b}$$

$$R_A=0\ , \tag{5.3c}$$

$$S=0=S_A\ . \tag{5.3d}$$

Figure 3 gives the hole subbands for the [110] growth axis. As in Fig. 1, there is no piezoelectric field in this

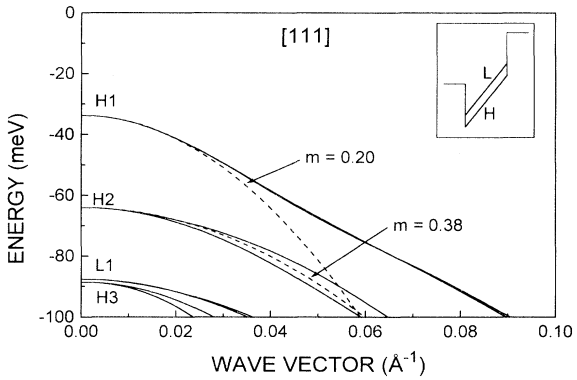

FIG. 2. Energy of the valence subbands in the axial approximation for a quantum well whose growth axis is [111]. The other parameters are the same as in Fig. 1. In this quantum well the piezoelectric field is 1.2 meV/Å. Hn, Ln, and V_L-V_H have the same meaning as in Fig. 1. The splitting V_L-V_H is 32.2 meV. There are two subbands for each Hn and Ln because there is no inversion center due to the piezoelectric field. The masses $m=0.20$ and $m=0.38$ are obtained by fitting the $H1$ and $H2$ hole subbands up to about 0.02 Å^{-1}. The so-called diagonal mass is 0.15 for heavy holes and 0.34 for light holes.

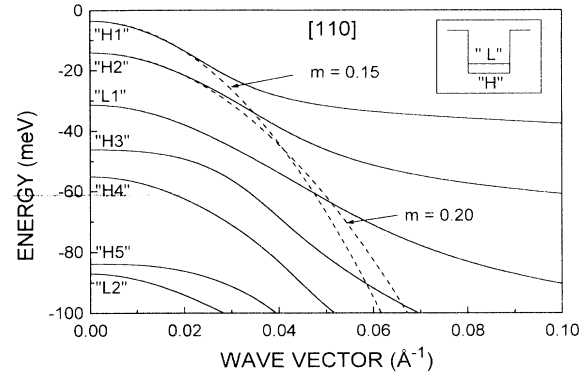

FIG. 3. Energy of the valence subbands in the axial approximation for a quantum well whose growth axis is [110]. The other parameters are the same as in Fig. 1. This quantum well has no piezoelectric field. "Hn" and "Ln" indicate that, even at $k_{\parallel}=0$, the functions are not pure $|\frac{3}{2}\pm\frac{3}{2}\rangle$ and $|\frac{3}{2}\pm\frac{1}{2}\rangle$: this is due to the fact that the Bir-Pikus Hamiltonian is not diagonal. The splitting V_L-V_H would be 30.5 meV if the off-diagonal R element of the Bir-Pikus Hamiltonian could be neglected. (Here $R=-3.1$ meV.) The masses $m=0.15$ and 0.20 are obtained by fitting the $H1$ and $H2$ hole subbands up to about 0.02 Å^{-1}. The so-called diagonal mass, which could be defined from Eq. (5.3a), is 0.15 for "heavy" holes and 0.33 for "light" holes.

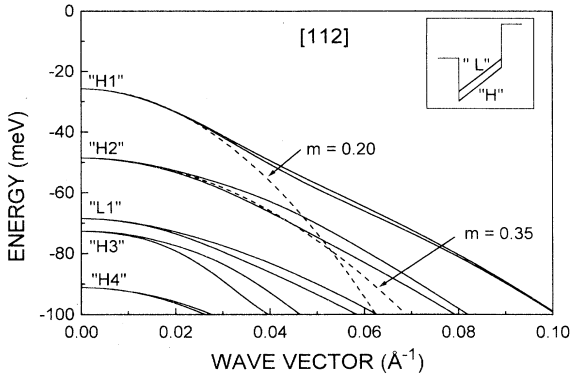

FIG. 4. Energy of the valence subbands in the axial approximation for a quantum well whose growth axis is [112]. The other parameters are the same as in Fig. 1. In this quantum well the piezoelectric field is 0.7 meV/Å. "Hn" and "Ln" have the same meaning as in Fig. 3. There are two subbands for each Hn and Ln as there is no inversion center due to the piezoelectric field. The splitting V_L-V_H would be 30.5 eV if the off-diagonal R and S elements of the Bir-Pikus Hamiltonian could be neglected. (Here $R=1.8$ meV and $S=-2.0$ meV.) The masses $m=0.20$ and 0.35 are obtained by fitting the $H1$ and $H2$ hole subbands up to about 0.02 Å^{-1}. The so-called diagonal masses, which could be defined from Eq. (5.4a), are identical to those of the [110] case given in Fig. 3.

direction. However, contrary to the [001] case the Bir-Pikus Hamiltonian is not diagonal as Eq. (4.10b) shows: strictly speaking the notation H and L does not have the same meaning as in the [001] and [111] cases. At $k_{\parallel}=0$ the wave functions are obtained after a diagonalization; we call H and L the solutions that are, respectively, mainly $|\frac{3}{2}+-\frac{3}{2}\rangle$ and $|\frac{3}{2}\pm\frac{1}{2}\rangle$. The splitting V_L-V_H has no strict meaning. However, we may define a splitting V_L-V_H if we neglect off-diagonal elements in $H_{\rm BP}$. $V_L-V_H=30.5$ meV. The Bir-Pikus off-diagonal element is -3.1 meV. The masses are 0.15 and 0.20 for $H1$ and $H2$ subbands. If we define diagonal masses from Eq. (4.4a), we obtain $1/(\gamma_1\pm\gamma_{31})$ for these masses that, numerically, are equal to 0.15 and 0.33.

[112] direction:

$$P\pm Q=\tfrac{1}{2}(\gamma_1\mp 2\gamma_{31})k_z^2\ , \tag{5.4a}$$

$$R=(\sqrt{3}/6)\gamma_\delta k_z^2\ , \tag{5.4b}$$

$$S=(2/\sqrt{6})\gamma_\delta k_z^2\ , \tag{5.4c}$$

$$R_A=S_A=0\ . \tag{5.4d}$$

Figure 4 gives the hole subbands for a [112] growth axis. As in the [111] case there is a piezoelectric field (which induces a difference of 70 meV between the two sides of the quantum well) and as in the [110] case the Bir-Pikus Hamiltonian is not diagonal. Thus for "H," "L," and "V_L"-"V_H" we keep the definition given above. The masses are 0.20 and 0.35 for $H1$ and $H2$ subbands. As for the diagonal mass, Eq. (4.5a) leads to the same definition as for the [110] case and therefore to the same numerical value while the "parabolic" masses for $H1$ and $H2$ have changed.

We notice that $X=X_A$ ($X=P,Q,R,S$) in [001] directions as predicted and in [111] directions as it could be guessed but this is not true for other directions. Thus the axial approximation is not strictly exact in general for $k_{\parallel}=0$. (Numerically the difference is of the order of 1% in CdTe and usual semiconductors where $\gamma_3/\gamma_2-1<0.5$; for silicon where $\gamma_3/\gamma_2-1=2$, this difference is 10% for low-symmetry directions.) It is tempting to add the off-diagonal terms proportional to $\gamma_\delta k_z^2$ in order to restore the exactitude. However, it would be inconsistent to keep these terms and not the others, which may be of the same order of magnitude for $k_{\parallel}\neq 0$. Therefore we keep the axial approximation without alteration throughout the present paper.

B. Axial average and cyclotron resonance

It is clear that for the axial approximation, dropping the terms in t_M ($M>0$) which give rise to the warping, gives an average mass, which we call axial mass, in a given plane of a bulk semiconductor: this axial mass m_A is simply obtained with $k_z=0$.

In the (001) plane,

$$1/m_A=\gamma_1\pm\{[7(\gamma_2)^2+3(\gamma_3)^2+6\gamma_2\gamma_3]/4\}^{1/2}\ . \tag{5.5a}$$

In the (111) plane,

$$1/m_A=\gamma_1\pm\{[(\gamma_2)^2+7(\gamma_3)^2+4\gamma_2\gamma_3]/3\}^{1/2}\ . \tag{5.5b}$$

In the (110) plane or (112) plane,

$$1/m_A=\gamma_1\pm\{[31(\gamma_2)^2+111(\gamma_3)^2+114\gamma_2\gamma_3]/64\}^{1/2}\ . \tag{5.5c}$$

The sign + (−) corresponds to a light (heavy) hole.

One could imagine taking this mass m_A, which is an in-plane mass, as the cyclotron mass in a cyclotron experiment. We can consider how this mass m_A is related to the mass m_{CR} usually used in cyclotron resonance. m_{CR} in the general case was considered in Ref. 38. Here we wish only to relate m_A to m_{CR} in the simple case as considered in Refs. 39–41 where the magnetic field is low ($k_z=0$) and there is no stress.

To first order the mass m_{CR} can be written as[39,40]

$$\frac{1}{m_{CR}}=\gamma_1\pm\{2[(\gamma_2)^2+(\gamma_3)^2]\}^{1/2} \pm\varepsilon\frac{(\gamma_3)^2-(\gamma_2)^2}{\{2[(\gamma_2)^2+(\gamma_3)^2]\}^{1/2}}\ , \tag{5.6a}$$

where

$$\varepsilon=-\tfrac{1}{4}\ \text{ in (100) plane}\ , \tag{5.6b}$$

$$\varepsilon=\tfrac{1}{2}\ \text{ in (111) plane}\ , \tag{5.6c}$$

$$\varepsilon=\tfrac{5}{16}\ \text{ in (110) plane}\ . \tag{5.6d}$$

Now we can write Eq. (5.5) as

$$1/m_A=\gamma_1\pm\{2[(\gamma_2)^2+(\gamma_3)^2]+\varepsilon_1[(\gamma_3)^2-(\gamma_2)^2]+\varepsilon_2(\gamma_3-\gamma_2)^2\}^{1/2}\ , \tag{5.7a}$$

with

$$\varepsilon_1=-\tfrac{1}{2},\ \varepsilon_2=-\tfrac{3}{4}\ \text{ in the (001) plane}\ , \tag{5.7b}$$

$$\varepsilon_1=1,\ \varepsilon_2=-\tfrac{2}{3}\ \text{ in the (111) plane}\ , \tag{5.7c}$$

$$\varepsilon_1=\tfrac{5}{8},\ \varepsilon_2=-\tfrac{57}{64}\ \text{ in the (110) and (112) planes}\ . \tag{5.7d}$$

If we put $\varepsilon_2=0$, i.e., we neglect the second-order $(\gamma_3-\gamma_2)^2$ term, and we develop Eq. (5.7a) to first order in $\gamma_3-\gamma_2$, we find exactly Eq. (5.6a)–(5.6d). This means that Eqs. (5.6) and Eq. (5.7) are identical to first order.

To go beyond the first order, we focus on the (111) plane, rather than looking at the general case, which is very tedious. If we take the whole Hamiltonian (with $\gamma_\delta\neq0$) it is straightforward to see that there is *no* warping, as pointed out in Ref. 41. This gives an *exact* mass m:

$$1/m_{111\|}=\gamma_1\pm\{(\gamma_2)^2+3(\gamma_3)^2\}^{1/2}\ , \tag{5.8}$$

which is nothing but the cyclotron mass given in Ref. 39 (where the mass is equal to that of Ref. 40 to first order) and is not equivalent to the axial mass (the difference is of the order of percent in the case of CdTe but is more important, about 10%, in the case of silicon where $\gamma_3>3\gamma_2$). This shows that we must be careful when dealing with an average mass. In the (111) plane and for $k_z=0$ we deal with a very special case where there is no warping so that, strictly speaking, the axial mass is not an average mass contrary to, for example, the case of the (100) plane. However, one should not thereby deduce that the axial approximation is not suitable for the problem of an average energy in a 2D semiconductor (111) plane. If k_z is not zero there is again a warping. In this last case, which corresponds to a 2D semiconductor, we need a coherent approximation if we look for a description that does not depend on the direction of the wave vector $\mathbf{k}_\|$ in the plane [(111), $k_z\neq0$]: the axial approximation fulfills this condition. Incidentally we can note that the axial mass is exactly the same in the (110) and (112) planes: the same holds for the cyclotron mass.

In short we see there is a slight difference between the axial mass and the cyclotron mass, the latter is more accurate than the axial mass for $k_z=0$. However, as soon as $k_z\neq0$, only the axial mass corresponds to an average: it is the only one we can use if we look for an average as the density of states.

VI. NUMERICAL CALCULATION OF HOLE SUBBANDS

A. General framework

In Ref. 10 the authors project **H** on a Fourier basis $|f_j\rangle$. To sum up their method we take the example of the conduction band in a semiconductor where the only direction of interest is z and the effective mass m is not constant, $m=m(z)$. We write here $\gamma=\gamma(z)=1/m(z)$ and $V=V(z)$. A matrix element of the Hamiltonian $h=\frac{1}{2}p\gamma p+V$ is written as[10]

$$\langle f_i|h|f_j\rangle=-\tfrac{1}{2}[\langle f_i|\gamma|(d^2f_j/dz^2)\rangle+\langle f_i|(d\gamma/dz)|(df_j/dz)\rangle]+\langle f_i|V(z)|f_j\rangle\ . \tag{6.1}$$

It was shown[10] that this method takes into account the usual boundary conditions and furthermore can be used for the valence band. The matrix elements are analytic.

We use a variant of this method. (i) Using the Hermiticity of p we write the above matrix element as

$$\langle pf_i|\gamma|pf_j\rangle+\langle f_i|V(z)|f_j\rangle\ . \tag{6.2}$$

This emphasizes the symmetry of h ($h_{ij}=[h_{ji}]^+$) which is not evident in Eq. (6.1) and especially simplifies the matrix element calculation, in particular when γ is not a constant. (ii) the Fourier basis $|f_j\rangle$ is well suited to a superlattice. In principle for a single quantum well of width L_w it is enough to increase the period of the superlattice up to a period much larger than L_w to get back the energies of the quantum well. However, in practice the larger the period, the larger the dimension of the needed basis to describe the potential V, and thus the slower the convergence of the energy calculation. Thus we take a description suited to a single quantum well[42] where an infinite quantum well of width L is used to describe the single quantum well. Finally we take $|\varphi_j\rangle=[\sqrt{1/L}\,]\sin(j\pi z/L)$ as the basis. There is a final problem: which width L is the most suited to a given quantum well or more precisely which width L gives the lowest energy? Furthermore, is there a unique width L that gives the lowest energy whatever the level of interest? To illustrate this we take the "worst" case, namely, the [111] case where the potential is the most asym-

metric: as stated above, the piezoelectric field results in a potential that varies from 120 meV, higher than the well depth due to the valence band offset. In Fig. 5 the energies are calculated at the center of the Brillouin zone for L varying from L_w (here 100 Å) to $6L_w$. Figure 5 shows that each energy E_n decreases quickly down to a minimum $E_{\min,n}$ for $L=L_{\min,n}$ and increases very slowly after.

We take a basis whose dimension is $N=30$. With this basis we obtain $E_{\min,H1}=33.66$ meV for $L_{\min,H1}=165$ Å, $E_{\min,H2}=63.94$ meV for $L_{\min,H2}=185$ Å, $E_{\min,L1}=87.44$ meV for $L_{\min,L1}=425$ Å and $E_{\min,H3}=88.48$ meV for $L_{\min,H3}=225$ Å. Eventually we take a single value for $L=300$ Å; with this last value we get, respectively, 33.75, 64.04, 87.59, and 88.55 meV, which are to be compared to the exact values 33.64, 63.92, 87.41, and 88.43 meV. Keeping $L=300$ Å we have checked that the accuracy is the same for $k_{\parallel}\neq 0$ (had we taken $N=100$ and $L=500$ Å the accuracy would have been better than 0.02 meV for the four levels whatever $k_{\parallel}$). This result, namely, one width L for all levels regardless of $k_{\parallel}$, is the crucial point of the method. This allows the study of any structure.

Finally we consider the limits of this variational calculation. It is beyond the scope of this paper to discuss in detail the limits of this method; we give here some brief indication. If the Luttinger parameters are not the same inside the well and in the barrier it is enough to increase the dimension N of the basis $|\varphi_j\rangle$. Typically for $Ga_{0.65}Al_{0.35}As$-GaAs-$Ga_{0.65}Al_{0.35}$ an accuracy of 0.1 meV is obtained with $N=50$. If there is a negative mass, typically a HgTe well inside CdTe barriers, the basis $|\varphi_j\rangle$ gives negative eigenvalues (i.e., energies below the bottom of the quantum well) if $L\leq L_w$ and these eigenvalues increase in magnitude as j becomes larger; this results from the fact that for $L\leq L_w$ the boundary conditions are not taken into account in Eq. (6.2) and in such a case the variational principle is not applicable with trigonometric functions; the results have no meaning. On the contrary, in direct-gap semiconductors such as CdTe or GaAs the results do not contain any spurious solutions and are reliable.

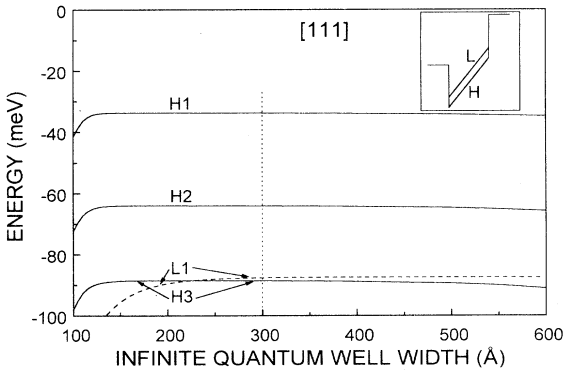

FIG. 5. This figure shows the energies at $k_{\parallel}=0$ of the bounded levels in a $Cd_{0.8}Mn_{0.2}Te$-CdTe-$Cd_{0.8}Mn_{0.2}Te$ quantum well where the growth axis is [111] vs the width L of an infinite quantum well whose eigenfunctions are the basis for the Hamiltonian. The width of the CdTe quantum well is $L_w=100$ Å. For L larger than 200 Å the energies vary very slowly. This figure is obtained with a basis of dimension $N=30$ and taking $L=300$ A: the energies have an accuracy of 0.1 meV, the accuracy of all the figures of this paper. Had we taken $N=100$, the accuracy would have been 0.01 meV.

B. Broido-Sham transformation

The Broido-Sham transformation[7] (BST), although not absolutely necessary, is a very convenient means of saving time in computer calculation (typically a coefficient of the order of 4^3). Here the purpose is, first, to show the practical limits of the BST independently of any considerations about the mathematical validity already discussed in Refs. 8, 16, and 18 and, second, to extend the application of BST to directions other than [001].

In the BST the following unitary matrix is used:

$$U=\begin{bmatrix} a^* & 0 & 0 & -a \\ 0 & b^* & -b & 0 \\ 0 & b^* & b & 0 \\ a^* & 0 & 0 & a \end{bmatrix}, \tag{6.3}$$

so that the matrix UH_LU^+ is

$$\begin{array}{cccc} |H-\rangle & |L-\rangle & |L+\rangle & |H+\rangle \end{array}$$

$$\begin{bmatrix} P+Q & R^- & 0 & 0 \\ R^+ & P-Q & 0 & 0 \\ 0 & 0 & P-Q & R^- \\ 0 & 0 & R^+ & P+Q \end{bmatrix}, \tag{6.4}$$

with

$$|H\pm\rangle = a|\tfrac{3}{2}\rangle \pm a^*|-\tfrac{3}{2}\rangle , \tag{6.5a}$$

$$|L\pm\rangle = b|-\tfrac{1}{2}\rangle \pm b^*|\tfrac{1}{2}\rangle , \tag{6.5b}$$

where $|m\rangle \equiv |\frac{3}{2}m\rangle$ and

$$R^{\pm}=|R|\pm i|S|, \quad R_A^{\pm}=|R_A|\pm i|S_A| . \tag{6.6}$$

Equation (6.4) is obtained for values of a and b we shall determine. We write

$$a=(1/\sqrt{2})\exp i\alpha, \quad b=(1/\sqrt{2})\exp i\beta , \tag{6.7}$$

where α and β are to be defined. If we write

$$R=|R|\exp i\rho, \quad S=|S|\exp i\sigma , \tag{6.8}$$

a straightforward calculation shows that α and β are equal to

$$\alpha=\pi/4+(\sigma+\rho)/2, \quad \beta=\pi/4+(\sigma-\rho)/2 . \tag{6.9}$$

This shows that the BST always works for any direction $[hkl]$ in a bulk semiconductor, where α and β have a single definition. We can take an example with [001] and

$$\mathbf{k}=(k\sin\theta\cos\varphi, k\sin\theta\sin\varphi, k\cos\theta) , \tag{6.10}$$

where θ and φ are the usual angles in spherical coordinates when Ox, Oy, Oz are, respectively, parallel to [100], [010], [001]. It is now straightforward to get

$$\sigma = -\varphi \ , \tag{6.11a}$$

$$\rho = \pi + \psi \ , \tag{6.11b}$$

with

$$\tan\psi = -[(\bar{\gamma}+\gamma_\delta)\sin 2\varphi]/[(\bar{\gamma}-\gamma_\delta)\cos 2\varphi] \ , \tag{6.12}$$

which allows one to find

$$\alpha = 3\pi/4 + (\psi - \varphi)/2 \ , \tag{6.13a}$$

$$\beta = -\pi/4 - (\psi + \varphi)/2 \ , \tag{6.13b}$$

and completely solves the problem in the [001] case.

Equation (6.9) in the general case and Eqs. (6.11)–(6.13) in the [001] case show that ψ depends on the parameters γ_2 and γ_3: in the usual case where the Luttinger parameters are not the same in the quantum well and in the barrier, so that α and β depend on the position, the functions (6.5) are not defined and the transformation is not possible. However, in the axial approximation, where $\gamma_\delta = 0$, ψ is merely equal to -2φ in the [001] case so that

$$\alpha = 3\pi/4 - 3\varphi/2 \ , \tag{6.14a}$$

$$\beta = -\pi/4 + \varphi/2 \ . \tag{6.14b}$$

The same result holds for other growth directions. This shows that the BST is always possible in the axial approximation used throughout this paper as far as the Luttinger Hamiltonian is concerned.[43] In the general case (without axial approximation) we have to resort to Eq. (6.13) and the BST is not usable. However, if we do not insist on mathematical rigor we can use the BST as in Ref. 18.

If now we add the Bir-Pikus Hamiltonian to the Luttinger Hamiltonian the problem becomes more complex. This problem was addressed in Ref. 16 from which it is easy to deduce that, in addition to the above results, the BST is feasible if the ε_{ij} are zero ($i \neq j$). As quoted in Ref. 16 this condition is fulfilled in [001] and [111] directions. We have seen that this condition holds for the [110] direction but not for the [112] direction. We can note that the BST is all the more useful in that it transforms a 4×4 complex matrix into two 2×2 real matrices. If the quantum well is symmetric these two matrices have identical eigenvalues and, as quoted above, the gain in computer time is of the order of 4^3. Even if the quantum well is not symmetric the gain is of the order of about thirty. Finally we can note that if we try to use the BST without taking into account the validity conditions two cases are possible; in the first we obtain a real 2×2 matrix; in the second (at least one of ε_{ij} does not equal zero for $i \neq j$) the 2×2 matrix has matrix elements that are (via $k_z \rightarrow -i\,d/dz$) pseudodifferential operators[44] and the problem to solve is much more complicated than the one we had at the beginning. We can make two remarks: first, in a bulk unstrained semiconductor one can always use the BST (this is rigorous from a mathematical viewpoint) and one could think of using it to solve the problem of acceptors: however, in this case the 2×2 matrix also contains pseudodifferential operators and the new problem is again more complicated than the initial problem; second in a one-dimensional semiconductor where $k_x \rightarrow -i\,d/dx$, $k_y \rightarrow -i\,d/dy$ (z parallel to the wire) the 2×2 matrix contains once again pseudodifferential operators. Finally we note that the efficiency of the BST is mainly due to the fact that only one component of the wave vector $\mathbf{k}$ (namely, k_z) is changed into an operator; if two components are to be changed the BST is not efficient.

We give now the matrix elements of $H_L + H_{\rm BP}$ after the BST, i.e., in the shape of Eq. (6.4), in the axial approximation used in this paper but it is straightforward to get them in the general case. The diagonal elements being identical to the ones given above, we give only the off-diagonal elements.

[001] direction:

$$R_A^{\pm} = (\sqrt{3}/2)\bar{\gamma}(k_\parallel)^2 \pm \sqrt{3}\gamma_3 k_\parallel (d/dz) \ ;$$

[111] direction:

$$R_A^{\pm} = (\sqrt{3}/2)\gamma_{21}(k_\parallel)^2 \pm \sqrt{3}\gamma_{12} k_\parallel (d/dz) \ ;$$

[110] direction:

$$R_A^{\pm} = |-(\sqrt{3}/2)\gamma_{53}(k_\parallel)^2 + (\sqrt{3}/2)\beta_\delta \varepsilon_{\parallel\perp}| \pm \sqrt{3}\bar{\gamma} k_\parallel (d/dz) \ .$$

C. Parameters

As said above we take the following parameters: the width L_w of the quantum well is 100 Å and the percentage of the manganese in the barrier is 20%.

Now we state the CdTe parameters.[45] The cell parameters are $a(Cd_{1-x}Mn_xTe) = 6.487 - 0.148x$ (Å) (after Ref. 46). The band-gap difference[46] between $Cd_{1-x}Mn_xTe$ and CdTe is $1592x$ (meV). The valence band offset[47] $\Delta E_v/\Delta E_G$ is 30%. The elastic stiffness constants[48] are $C_{11} = 5.66$, $C_{12} = 3.96$, $C_{44} = 2.07$ (in 10^{10} Pa). In the Bir-Pikus Hamiltonian, the hydrostatic deformation potential is $a = 1.1$ eV and the shear deformation potentials are $b = 1.1$ eV and $d = 3.3$ eV.[49]

As for the Luttinger parameters there are strong discrepancies in the literature. For example, $\gamma_2 = 1.7 \pm 0.3$ in Ref. 41 and 1.08 ± 0.15 in Ref. 50. Here we take the values given in Ref. 51 where a detailed discussion based on the comparison of results obtained by cyclotron resonance and in wide quantum well is given; a consistent set of parameters is $\gamma_1 = 4.8$, $\gamma_2 = 1.5$, $\gamma_3 = 1.9$.

However, due to the uncertainty of the values of the Luttinger parameters in CdTe and considering that the Luttinger parameters of CdMnTe are still less well known, it seems to us unreasonable to take different parameters inside and outside the quantum well and thus we take the Luttinger parameters of CdTe for CdMnTe also.

Finally we must take into account the piezoelectric

field $\mathcal{E}$. In principle it is possible to link $\mathcal{E}$ and the piezoelectric coefficient e_{14} by a linear relation via the C_{ij}. However, it was shown both experimentally[24] and theoretically[25] that e_{14} is not constant in CdTe even to a first approximation and therefore we have preferred to simply use the experimental value of $\mathcal{E}$.[24] Thus we take $\mathcal{E}=0$ for the growth axis in the [001] and [110] directions, $\mathcal{E}=1.2$ meV/Å in the [111] direction, and $\mathcal{E}=0.7$ meV/Å in the [112] direction. The accuracy of these parameters is discussed in Refs. 24 and 25.

VII. CONCLUSION

We have extended previous calculations of hole subbands in quantum well semiconductors to cover explicitly all the $[hhk]$ growth directions in strained semiconductors. Furthermore, the numerical method used here allows one to recover all of the cases of "positive" gap known by the author. We have given examples in four characteristic directions. We have shown the possibilities and the limits of the Broido-Sham transformation. We have discussed in detail the validity of the axial approximation and its connection to the cyclotron mass. Finally we have given the tensors that allow one to get both the Luttinger and Bir-Pikus Hamiltonians and to extract their axial parts if needed.

ACKNOWLEDGMENTS

I thank Claudine Hermann for efficient hints about the Broido-Sham transformation, Maurice Lombardi for illuminating advice about all of the mathematical aspects of this paper, Régis André for enlightening discussions about strained semiconductors and more particularly of the behavior on piezoelectric coefficient in CdTe, Le Si Dang and Robert Romestain for stimulating discussions about the link between axial and cyclotron mass, Massimo Altarelli for pertinent remarks about the axial approximation, and Gavin Vaughan for a critical reading of the manuscript. I acknowledge also useful discussions with Denis Bertho, Dirk Brinkmann, Bernard Gil, Axel Haury, and Christian Jouanin.

APPENDIX

This appendix gives the tensors t_M and τ_M used to describe, respectively, the Luttinger Hamiltonian and the Bir-Pikus Hamiltonian. All these tensors have the shape given by Eq. (2.1). They have vanishing trace: $P=0$. Thus it is sufficient to know three terms, Q, R, and S, in order to know a tensor.

t_M tensors

We write $\chi=k_{\parallel}^2-2k_z^2$.

For t_s:

$$Q=\tfrac{1}{2}\chi,\quad R=-\tfrac{1}{2}\sqrt{3}k_-^2,\quad S=\sqrt{3}k_-k_z\ .$$

For t_0:

$$Q=-3\chi,\quad R=\tfrac{1}{2}\sqrt{3}k_-^2,\quad S=4\sqrt{3}k_-k_z\ .$$

For t_1:

$$Q=-(6/\sqrt{14})k_xk_z,\quad R=(\sqrt{3/14})k_-k_z\ ,$$

$$S=-(\sqrt{3/14})(\chi+k_-^2/2)\ .$$

For t_2:

$$Q=[3/(2\sqrt{7})](k_x^2-k_y^2)\ ,$$

$$R=-[\sqrt{3}/(2\sqrt{7})]\chi,\quad S=-2[\sqrt{3/7}]k_+k_z\ .$$

For t_3:

$$Q=0,\quad R=-(\sqrt{3/2})k_+k_z\ ,$$

$$S=\tfrac{1}{2}(\sqrt{3/2})k_+^2\ .$$

For t_4:

$$Q=0,\quad R=(\sqrt{3}/2)k_+^2,\quad S=0\ .$$

τ_M tensors

To get τ_M it is enough to replace k_ik_j in t_M by ε_{ij}. We give the τ_M for convenience.

We recall that $\varepsilon_{\parallel\perp}=\varepsilon_{\parallel}-\varepsilon_{\perp}$, $\varepsilon_{\perp}=\varepsilon_{zz}$.

For τ_s:

$$Q=\varepsilon_{\parallel\perp},\quad R=0,\quad S=\sqrt{3}\varepsilon_{xz}\ .$$

For τ_0:

$$Q=-6\varepsilon_{\parallel\perp},\quad R=0,\quad S=4\sqrt{3}\varepsilon_{xz}\ .$$

For τ_1:

$$Q=-3(\sqrt{2/7})\varepsilon_{xz},\quad R=(\sqrt{3/14})\varepsilon_{xz}\ ,$$

$$S=-(\sqrt{6/7})\varepsilon_{\parallel\perp}\ .$$

For τ_2:

$$Q=0,\quad R=-(\sqrt{3/7})\varepsilon_{\parallel\perp},\quad S=-2(\sqrt{3/7})\varepsilon_{xz}\ .$$

For τ_3:

$$Q=0,\quad R=-(\sqrt{3/2})\varepsilon_{xz},\quad S=0\ .$$

For τ_4:

$$Q=R=S=0\ .$$

[1]S. S. Nedorezov, Sov. Phys. Solid State **12**, 1814 (1971).
[2]E. Bangert and G. Landwehr, Surf. Sci. **58**, 138 (1976).
[3]J. M. Luttinger, Phys. Rev. **102**, 1030 (1956).
[4]S. R. White and L. J. Sham, Phys. Rev. Lett. **47**, 879 (1981).
[5]G. Bastard, Phys. Rev. B **24**, 5693 (1981).
[6]M. Altarelli, Phys. Rev. B **28**, 842 (1983).
[7]D. A. Broido and L. J. Sham, Phys. Rev. B **31**, 888 (1985).
[8]A. Twardowski and C. Hermann, Phys. Rev. B **35**, 8144 (1987).
[9]R. Eppenga, M. F. H. Schurman, and S. Colak, Phys. Rev. B **36**, 1554 (1987).
[10]G. A. Baraff and D. Gershoni, Phys. Rev. B **43**, 4011 (1991).
[11]M. G. Burt, J. Phys. Condens. Matter **4**, 6651 (1992).
[12]B. A. Foreman, Phys. Rev. B **48**, 4964 (1993).
[13]G. Goldoni, Ph.D. thesis, Trieste, 1993.
[14]G. Platero and M. Altarelli, Phys. Rev. B **36**, 6591 (1987).
[15]J. Lee, C. Jagannath, M. O. Vassel, and E. S. Koteles, Phys. Rev. B **37**, 4164 (1988).
[16]J. Lee and M. O. Vassel, Phys. Rev. B **37**, 8855 (1988).
[17]L. C. Andreani, A. Pasquarello, and F. Bassani, Phys. Rev. B **36**, 5887 (1987).
[18]B. A. Foreman, Phys. Rev. B **49**, 1757 (1994).
[19]D. L. Smith and C. Mailhiot, Phys. Rev. Lett. **58**, 1264 (1987); Rev. Mod. Phys. **62**, 173 (1990).
[20]G. E. Pikus and G. L. Bir, Sov. Phys. Solid State **1**, 136 (1959).
[21]G. Goldoni and A. Fasolino, Phys. Rev. Lett. **69**, 2567 (1992); **70**, 2051 (1993).
[22]P. Lefebvre, P. Bonnel, B. Gil, and H. Mathieu, Phys. Rev. B **44**, 5635 (1991).
[23]R. André, C. Bodin, J. Cibert, L. S. Dang, and G. Feuillet, J. Phys. IV (France) **3**, 429 (1993).
[24]R. André, Ph.D. thesis, Université J. Fourier-Grenoble 1, 1994.
[25]A. Dal Corso, R. Resta, and S. Baroni, Phys. Rev. B **47**, 16 252 (1993).
[26]E. C. Valadares, Phys. Rev. B **46**, 3935 (1992).
[27]R. K. Hayden, E. C. Valadares, M. Henini, L. Eaves, D. K. Maude, and J. C. Portal, Phys. Rev. B **46**, 15 586 (1992); **49**, 8501 (1993).
[28]R. Nötzel and K. Ploog, Phys. Rev. B **49**, 8499 (1994).
[29]M. Altarelli, U. Ekenberg, and A. Fasolino, Phys. Rev. B **32**, 5138 (1985).
[30]N. O. Lipari and M. Altarelli, Phys. Rev. B **15**, 4883 (1977).
[31]G. Dresselhaus, Phys. Rev. **100**, 580 (1955).
[32]G. L. Bir and G. E. Pikus, Sov. Phys. Solid State **3**, 2221 (1962); R. Ranvaud, H. R. Trebin, U. Rössler, and F. H. Pollak, Phys. Rev. B **20**, 701 (1979); C. Priester and M. Lannoo, *ibid.* **19**, 10 559 (1991); M. Silver, W. Batty, A. Ghiti, and E. P. O'Reilly, *ibid.* **46**, 6781 (1992).
[33]A. Baldereschi and N. O. Lipari, Phys. Rev. B **8**, 2697 (1973).
[34]A. Messiah, *Mecanique Quantique* (Dunod, Paris, 1995), pp. 918–926.
[35]Y. Tanabe and H. Kamimura, J. Phys. Soc. Jpn. **13**, 394 (1958). This paper gives the Clebsch-Gordan coefficients, which allows one to find the usual Luttinger Hamiltonian quantized symmetrically with respect to $(1\bar{1}0)$ plane along a [001] direction as well as the one quantized along a [111] direction.
[36]E. Anastassakis, J. Appl. Phys. **68**, 4561 (1990).
[37]The results of Refs. 24 and 36 are fully compatible. The results of Ref. 36 are quite general while those of Ref. 24 are given in the case of interest here, namely, axes x and z in the $(1\bar{1}0)$ plane. The derivation of the results of Ref. 24 from those of Ref. 36 requires a tedious calculation. Thus we give here the results of Ref. 24, which are not easily accessible.
[38]J. C. Hensel and K. Suzuki, Phys. Rev. B **9**, 4219 (1974).
[39]G. Dresselhaus, A. F. Kip, and C. Kittel, Phys. Rev. **98**, 368 (1955).
[40]H. J. Zeiger, B. Lax, and R. N. Dexter, Phys. Rev. **105**, 495 (1957).
[41]Le Si Dang, G. Neu, R. Romestain, Solid State Commun. **44**, 1187 (1982).
[42]D. Gershoni, H. Temkin, G. J. Dolan, J. Dunsmuir, S. N. G.Chu, and M. B. Panish, Appl. Phys. Lett. **53**, 995 (1988).
[43]Equations (6.14) were obtained in Ref. 8 where unfortunately there are some misprints.
[44]L. Hörmander, Acta. Math. **127**, 79 (1971); J. Duistermaat and L. Hörmander, *ibid.* **128**, 183 (1971); J. Duistermaat, *Fourier Integral Operators* (Courant Institute of Mathematical Sciences, New York, 1973).
[45]The values used here are taken from a thorough discussion given in Ref. 24 using Refs. 46–50.
[46]J. K. Furdyna, J. Appl. Phys. **64**, R29 (1988).
[47]A. Wasiela, P. Peyla, Y. Merle d'Aubigné, J. E. Nicholls, D. E. Ashenford, and B. Lunn, Semicond. Sci. Technol. **7**, 571 (1992).
[48]R. D. Greenough and S. B. Palmer, J. Phys. D **6**, 587 (1973). The elastic stiffness constants given here are extrapolated at $T=0$ K.
[49]D. J. Olego, J. Petruzzelo, S. K. Ghandi, N. R. Taskar, and I. B. Bhat, Appl. Phys. Lett. **51**, 127 (1987); H. Mathieu, J. Allegre, A. Chatt, P. Lefebvre, and J. P. Faurie, Phys. Rev. B **38**, 7740 (1988); G. Gil and D. J. Dunstan, Semicond. Sci. Technol. **6**, 428 (1991); Y. Merle d'Aubigné, H. Mariette, N. Magnea, H. Tuffigo, R. T. Cox, G. Lentz, Le Si Dang, J. L. Pautrat, and A. Wasiela, J. Cryst. Growth **101**, 650 (1990).
[50]Ch. Neumann, A. Nöthe, and N. O. Lipari, Phys. Rev. B **37**, 922 (1988).
[51]Le Si Dang (unpublished).